Robust Design Optimization of Electrical Machines: A Comparative Study and Space Reduction Strategy

Gang Lei, *Member, IEEE,* Gerd Bramerdorfer, *Senior Member, IEEE,* Chengcheng Liu, Youguang Guo, *Senior Member, IEEE,* and Jianguo Zhu, *Senior Member, IEEE*

***Abstract*—This paper presents a comparative study on different types of robust design optimization methods for electrical machines. Three robust design approaches, Taguchi parameter design, worst-case design and design for six-sigma, are compared for low-dimensional and high-dimensional design optimization scenarios, respectively. For the high-dimensional scenario, the computational burden is normally massive due to the robustness evaluation of a huge number of design candidates. To attempt this challenge, as the second aim of this paper, a space reduction optimization (SRO) strategy is proposed for these robust design approaches, yielding three new robust optimization methods. To illustrate and compare the performance of different robust design optimization methods, a permanent magnet motor with soft magnetic composite cores is investigated with the consideration of material diversities and manufacturing tolerances. 3-D finite element model and thermal network model are employed in the optimization process and the accuracy of both models has been verified by experimental results. Based on the theoretical analysis and optimization results, a detailed comparison is provided for all investigated and proposed robust design optimization methods in terms of different aspects. It shows that the proposed SRO strategy can greatly improve the design optimization effectiveness and efficiency of those three conventional robust design methods.**

***Index Terms*—Electrical machines, manufacturing tolerances, permanent magnet motor, robust design optimization, space reduction optimization, soft magnetic composite.**

I. Introduction

ELECTRICAL machines are the key components in many appliances, industrial equipment and systems. To improve their performance, such as higher torque density and efficiency and lower cost, different kinds of design optimization methods have been developed. These methods can be classified into two main approaches, deterministic and robust approaches, in terms of the consideration of uncertainties. The deterministic approach has dominated the field of design optimization of electrical machines for a long time [1-10].

Deterministic approach is able to provide an optimal design or a Pareto front (a set of non-dominated designs) for an electrical machine in a comparably short time or without high computation cost in many situations. For instance, this holds for optimizing a permanent magnet (PM) motor with 3-5 structural parameters using a genetic algorithm and analyzing the design candidates by 2-D finite element models (FEM). However, the main problem of the deterministic approach is that it cannot handle uncertainties, such as material diversities and manufacturing tolerances, that widely exist in the manufacturing process of electrical machines. These uncertainties will bring significant variations (or low quality) of the performance of electrical machines [11-18].

To ensure the high manufacturing quality of the electrical machines in production, strict quality control and management methods can be applied, for example, six-sigma quality control. However, this requires extra resources and maybe a burden for small and medium-sized enterprises. In addition, the therewith associated additional cost are usually not accepted, in particular when dealing with mass-produced electric machines.

To solve this problem, robust design optimization methods have been developed to investigate the impact of potential uncertainties in the early development stage of products like electrical machines. The main purpose of robust design is to seek a design that is insensitive to the variations of design variables and preassigned parameters [2,3,13]. There are three popular approaches, the Taguchi parameter design, worst-case (WC) design and design for six-sigma (DFSS). They will be introduced and compared for the design optimization of electrical machines in this work.

However, there is a major challenge for the robust design optimization of electrical machines in the high-dimensional situation, i.e. the huge computation cost for the evaluation of robustness of many design candidates. To attempt this challenge, a space reduction optimization (SRO) strategy is proposed for all three robust design approaches. Then, a

---

G. Lei and Y. Guo are with the School of Electrical and Data Engineering, University of Technology Sydney, Ultimo, NSW 2007, Australia (e-mail: gang.lei@uts.edu.au).

G. Bramerdorfer is with the Department of Electrical Drives and Power Electronics, Johannes Kepler University Linz, Linz 4040, Austria (email: gerd.bramerdorfer@jku.at)

C. Liu is with the State Key Laboratory of Reliability and Intelligence of Electrical Equipment, Tianjin 300130, China. He is the corresponding author.

J. Zhu is with the School of Electrical and Information Engineering, University of Sydney, Camperdown, NSW 2006, Australia.

This work was supported in part by the State Key Laboratory of Reliability and Intelligence of Electrical Equipment under project No. EERIKF2018005, Hebei University of Technology.

comprehensive comparative study will be presented for all investigated design optimization methods in this work, including the conventional deterministic approach and the proposed new methods.

The remainder of this paper is organized as follows: Section II briefs the formulations of Taguchi parameter design, WC design and DFSS. Section III presents a comparative study of these three robust design optimization methods based on a design example. A PM motor with soft magnetic composite (SMC) cores is investigated with the consideration of different uncertainties. Section IV describes the proposed SRO strategy and applies it to the conventional robust design optimization methods. Section V investigates the example study again with more parameters and uncertainties to show the effectiveness of the proposed methods and to compare the performance of different robust methods, followed by the conclusion.

II. Robust Design Optimization Methods

A. Comparison of Deterministic and Robust Designs

Figure 1 shows a brief comparison of deterministic and robust designs. As shown, the objective value of deterministic optimum is smaller and thus better than that of the illustrated robust optimum. However, in the presence of a small variation (Δx), there is a big fluctuation to the objective value (Δf) of the deterministic design. Most importantly, some points in the fluctuation are over the limit of the design objective, which means unsatisfactory products in production. The main reason for this fact is that the deterministic approach (DA) tends to push the optimal design close to the boundary of the constraints, following a high risk of unsatisfactory designs or failures in the presence of uncertainties. A small variation due to imperfect materials or manufacturing will lead to a big unsatisfactory rate of the product in manufacturing/production. Consequently, a robust approach is very important for the industrial application of electrical machines, especially in the context of Industry 4.0, as both motor performance and production quality must be considered in the design process, which may benefit the flexible and small batch production or customized electrical machines.

B. Formulations of Deterministic and Robust Designs

Generally, a deterministic design with respect to an objective $f(\mathbf{x})$ and m constraints $g(\mathbf{x})$ has the form as

$$\begin{aligned} \min:\quad & f(\mathbf{x}) \\ \text{s.t.}\quad & g_j(\mathbf{x}) \le 0, j = 1,2,\dots,m \ , \\ & \mathbf{x}_l \le \mathbf{x} \le \mathbf{x}_u \end{aligned} \tag{1}$$

where $\mathbf{x}_l$ and $\mathbf{x}_u$ are the boundaries of the design parameter $\mathbf{x}$, and $\mathbf{x}$ does not include any uncertain information [3]. To consider the uncertainties, there are three popular robust design approaches, Taguchi parameter design [19-24], WC design [25-27], and DFSS [27-31].

Taguchi parameter design is a kind of statistical experimental method for the quality improvement of product/process by minimizing the effects of the uncertainties or variations [23]. Figure 2 shows a block diagram of a product/process design in the Taguchi method. As shown, there are control factors and noise factors. The noise factors represent the uncertainties that may be hard to or cannot be controlled by the designer.

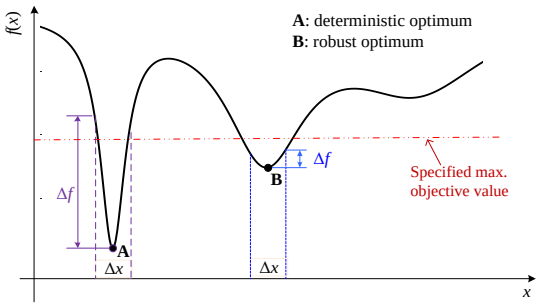

Fig. 1. Illustration and comparison of deterministic and robust designs.

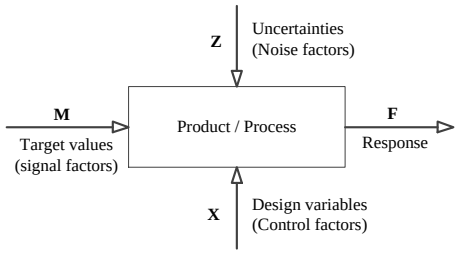

Fig. 2. Block diagram of a product/process design in Taguchi method

For the design of an electrical machine, material diversities and manufacturing tolerances can be considered as noise factors. When the target value of a response is given, like the output power or torque, the Taguchi design determines an optimal combination of control factor levels so that the variation of this response is minimized even though noise factors exist [24]. To implement the Taguchi design, an orthogonal array (OA) consisting of an inner array (formed with control factors with certain levels) and an outer array (formed with noise factors with certain levels) is required first. Then, the best factor-level combinations can be determined by signal-to-noise ratios (SNRs) based on the simulation data of the OA. SNRs can be classified into three types, nominal-is-best, larger-the-best, and smaller-the-best. As a minimum is sought in (1), the smaller-the-best type is considered in this work. The SNR of this type is defined as

$$\text{SNR} = -10\log\left(\frac{1}{n_s}\sum_{i=1}^{n_s} y_i^2\right), \tag{2}$$

where y_i is the response of $f(\mathbf{x})$ for n_s combinations of noise factors in the outer array. Other types of SNRs can be found in [23,24]. The Taguchi parameter design has been widely employed in many applications due to its efficiency and effectiveness. However, it has two main imperfections. First, the constraints are not formulated in this method while it is typically involved with optimization formulations of electrical machines, like the maximal volume, weight and temperature rise in the windings. Second, optimization is not generally performed, so the obtained Taguchi design depends on the designer's experience [28]. Fortunately, WC design and DFSS can handle both constraints and optimization aspects.

For WC robust approach, the design optimization model can be defined as

$$\begin{aligned} \min:\quad & f_w(\mathbf{x}) = \max_{\boldsymbol{\xi}\in U(\boldsymbol{\xi})} f(\mathbf{x},\boldsymbol{\xi}) \\ \text{s.t.}\quad & g_{w,j}(\mathbf{x}) = \max_{\boldsymbol{\xi}\in U(\boldsymbol{\xi})} g_j(\mathbf{x},\boldsymbol{\xi}) \le 0, j = 1,2,\dots,m \ , \\ & U(\boldsymbol{\xi}) = \{\boldsymbol{\xi} \in R^k \,|\, |\boldsymbol{\xi} - \boldsymbol{\xi}_n| \le \Delta\boldsymbol{\xi}\} \end{aligned} \tag{3}$$

where $\boldsymbol{\xi}$ and $\boldsymbol{\xi}_n$ stand for the vector and nominal values of

noise factors, respectively, $U(\boldsymbol{\xi})$ represents the uncertainty range. Please note that $\boldsymbol{\xi}$ may be different from the optimization parameter vector $\mathbf{x}$. For example, several structural parameters of a surface-mounted PM synchronous motor are optimized to reduce the variation of cogging torque due to the diversity of the PM remanence. Theoretically, WC robust approach is a minimax optimization problem. It uses the worst-case scenario, the worst performance of a design under uncertainties, as a measure of robustness. As it only investigates the worst-case scenario, the reliability of a design can be ensured, but the robustness is not considered in the implementation.

For DFSS robust approach, its design optimization model can be defined as

$$\begin{aligned} \text{min:} \quad & F[\mu_f(\mathbf{x}), \sigma_f(\mathbf{x})] \\ \text{s.t.} \quad & g_j[\mu_f(\mathbf{x}), \sigma_f(\mathbf{x})] \le 0,\ j = 1,2,\dots,m \\ & \mathbf{x}_l + n\boldsymbol{\sigma}_\mathbf{x} \le \boldsymbol{\mu}_\mathbf{x} \le \mathbf{x}_u - n\boldsymbol{\sigma}_\mathbf{x} \\ & \text{LSL} \le \mu_f \pm n\sigma_f \le \text{USL} \end{aligned}, \tag{4}$$

where μ and σ are the mean and standard deviation, respectively, and they are usually estimated by Monte Carlo analysis (MCA) method. LSL and USL are the lower and upper specification limits, respectively, such as the limits for output power and material cost. n is the sigma level. The value of n can be equivalent to a probability associated with the normal distribution, as shown in Fig. 3 and Table I [28,29]. For example, 3σ is equivalent to a percent of pass 99.73% or 2,700 defects per million opportunities (DPMO). However, this is only correct in terms of statistics or short-term quality control. For the long-term quality control, due to the shift (~1.5 σ) [28] in the mean (as shown in Fig. 3), 3σ quality is actually equivalent to 66,811 DPMO. Obviously, this is unacceptable for the batch production of products in the industry. Therefore, 6σ quality level has been widely adopted in industry, and its DPMO is only 3.4.

The main difference between WC and DFSS approaches is the probability distributions of noise factors. Normal distributions are always employed for the noise factors in DFSS, while WC approach does not require any information of the distributions. Thus, DFSS uses μ and σ as the measure of robustness, which is different from that of WC approach.

To compare the product's reliability by using different design approaches, a criterion called as probability of failure (PoF) has been used in many works [28,29]. It has the form as

$$\text{PoF} = 1 - \prod_{i=1}^{m} P(g_i \le 0) \tag{5}$$

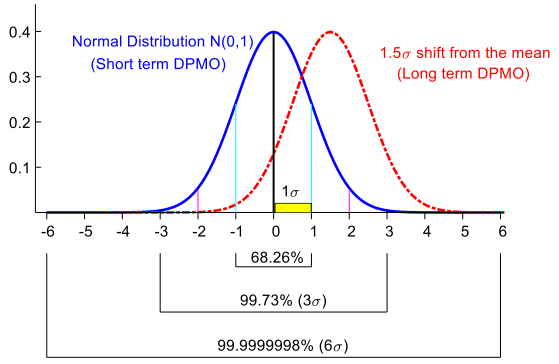

Fig. 3. Sigma level and its equivalent probability

TABLE I
PERCENTAGE AND DPMOS WITH RESPECT TO SIGMA LEVEL

Sigma level	Percentage	DPMO (short term)	DPMO (long term)
1	68.26	317,400	697,672
2	95.46	45,400	308,770
3	99.73	2,700	66,811
4	99.9937	63	6,210
5	99.999943	0.57	233
6	99.9999998	0.002	3.4

III. COMPARISON OF ROBUST DESIGN OPTIMIZATION METHODS

This section compares the performance of three robust design approaches introduced in Section II based on a design example of a PM claw pole motor (CPM) with SMC stator and NdFeB magnets. As a low-dimensional design example, four parameters are considered in the design optimization process.

A. Design Example Description

Figure 4 shows the design structure and parameters of the investigated motor. SMC powders are used to design and fabricate the stator (Fig. 4c) of this motor. Due to the unique 3-D magnetic characteristics of the SMC powders, this is a 3-D flux motor. The advantages of using SMC material in PM motors can be found in [32-34]. This motor initially was designed to provide a rated output power of 500 W at rated speed 1800 rev/min featuring an efficiency of 81.5% [35,36]. Table II lists some initial design parameters of this motor. The optimization model is defined as,

$$\begin{aligned} \text{min:} \quad & f(\mathbf{x}) = w_1 \frac{Cost}{Cost\_initial} + w_2 \frac{P_{out\_initial}}{P_{out}} \\ & g_1(\mathbf{x}) = 500 - P_{out} \le 0 \\ & g_2(\mathbf{x}) = 0.815 - \eta \le 0 \\ \text{s.t.} \quad & g_3(\mathbf{x}) = sf - 0.7 \le 0 \\ & g_4(\mathbf{x}) = T_{coil} - 75 \le 0 \\ & g_5(\mathbf{x}) = T_{pm} - 75 \le 0 \\ & \mathbf{x}_l \le \mathbf{x} \le \mathbf{x}_u \end{aligned}, \tag{6}$$

where *Cost* and P_{out} are the motor's material cost and output power, respectively, η, sf, T_{coil}, and T_{pm} are the motor efficiency, slot filling factor, temperature rise in the winding, and temperature rise in the PM, respectively. w_1 and w_2 are weighting factors and they will affect the optimal results. As both cost and output power are normalized and there is no preference, they are defined as 1 in this work. Table III lists the four design parameters and their ranges. They are considered as both control factors and noise factors in this example study.

Figure 5 shows a prototype of the SMC stator. It is made by molding instead of lamination technology. Figure 6 shows the experimental platform and the measured efficiency, input power and output power. For the analysis and calculation of the motor performance, a 3-D finite element model (FEM) and a 3-D thermal network model are applied [35]. Figure 7a shows a no-load flux density distribution based on the 3-D FEM. Figure 7b shows the 3-D thermal network model for the middle stack of the studied PM CPM.

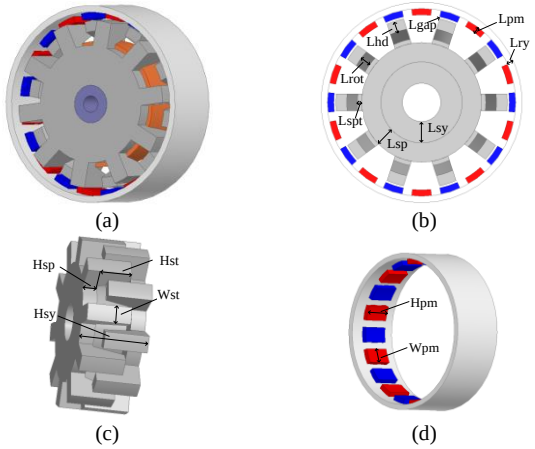

Fig. 4. 3D design structure and parameters of the PM CPM

TABLE II
INITIAL DESIGN OF THE CPM

Par.	Description	Unit	Value
L_{pm}	Length of PM	mm	3
W_{st}	tooth circumferential width	mm	10
W_{pm}	PM circumferential width	deg	12
H_{sy}	Height of stator yoke	mm	31
H_{sp}	Height of stator plate	mm	8
H_{st}	Height of tooth	mm	14.35
H_{pm}	Height of PM	mm	8
D	Diameter of copper wire	mm	1.1
N	Turns of coil	-	70
L_{gap}	Length of air gap	mm	1
B_r	PM remanence	T	1.15
ρ	SMC core density	g/mm^3	7.32

TABLE III
DESIGN PARAMETERS AND RANGES FOR LOW-DIMENSIONAL CASE

Par.	Unit	Initial	Min	Max	Step Size
W_{pm}	deg	12	10	14	0.05
H_{pm}	mm	15	11	17	0.05
N	turns	75	60	100	1
D	mm	1.1	0.9	1.5	0.01

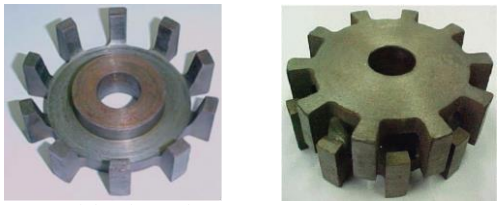

Fig. 5. Prototype of the claw pole stator.

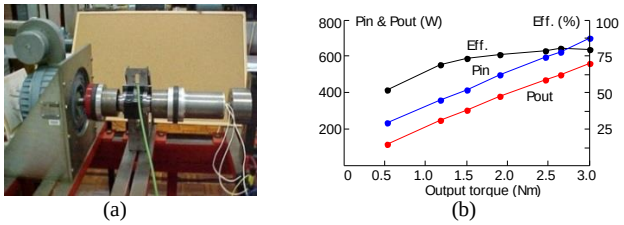

Fig. 6. (a) Test platform of the CPM, and (b) measured power and efficiency

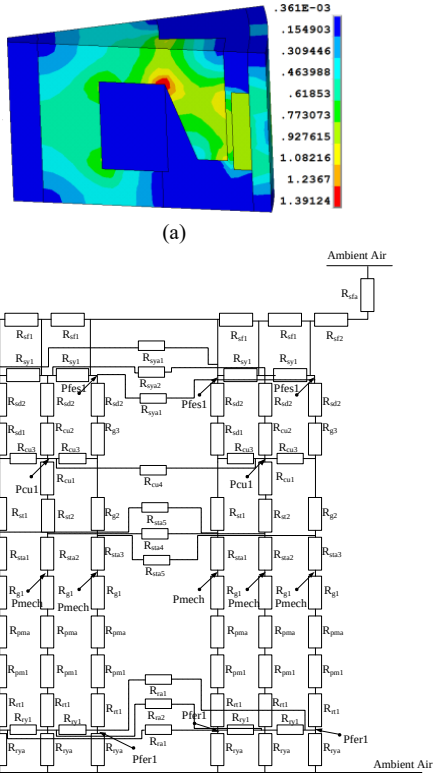

Fig. 7. (a) No-load flux density distribution computed using a 3-D FEM, and (b) a nodal thermal structure for 3-D heat flow

TABLE IV
KEY PARAMETERS VALIDATION OF THE INITIAL DESIGN OF PM CPM

Par.	Unit	Calculated	Measured	Relative error
Back EMF constant	V/rpm	0.0272	0.0271	-0.37%
No load core loss	W	58	60	+3.33%
Cogging torque peak	Nm	0.35	0.33	-6.06%
Coil temperature rise	℃	74	71	-4.23%

The two side stacks can be neglected, as the temperature of the middle stack is higher than that of the two side stacks. The thermal resistances of the conduction in this section are calculated as follows: one segment of the stator yoke is divided into two parts (R_{sy1}); stator side disk (R_{sd1} and R_{sd2}); coils (R_{cu1}, R_{cu2}, and R_{cu3}); stator claw pole teeth (R_{st1}, R_{st2}); air gaps into different position (R_{g1}, R_{g2}, R_{g3}); PMs (R_{pm1}); rotor in radial direction (R_{rt1}); rotor in axial direction(R_{ry1}); and shaft (R_{sf1} and R_{sf2}). (R_{sta1}, R_{sta2}, R_{sta3}), R_{cua}, R_{pma}, R_{rta}, and R_{sfa} are the equivalent thermal resistances between the air and stator teeth, stator disk, coil, PMs, rotor, and shaft, respectively. The thermal resistances in the circumference direction in this motor are calculated as: stator yoke (R_{sya1} and R_{sya2}); coil (R_{cu4}); stator teeth (R_{sta4} and R_{sta5}); and rotor (R_{ra1} and R_{ra2}). The heat sources in this model include the stator core loss, rotor core loss, copper loss, and mechanical loss. In order to gain a relatively high accuracy, each loss component is subdivided into several parts. The stator core loss is divided into six parts (P_{Fes1}), the copper loss is divided into two parts (P_{cu1}), the rotor core loss is divided into four parts (P_{Fer1}), and the mechanical loss is divided into six parts (P_{mech1}).

Table IV tabulates several calculated and measured motor performance parameters. For the back EMF constant, no-load core loss and temperature rise in the winding, the relative errors between calculated and measured values are less than 5%. For the accurate calculation of core loss in this PM-SMC motor, both alternating and rotational core losses are included [32,34]. Therefore, both the 3-D FEM and 3-D thermal network model are of good accuracy and it is reliable to use them in the following optimization.

B. Optimization Process and Results of Taguchi Approach

The implementation of Taguchi parameter design approach includes the following four main steps:

Step 1: Develop an OA consisting of an inner array and an outer array. The inner array and outer array are determined by the control factors and noise factors, respectively. Tables V and VI list the control factors and noise factors and their levels for this motor, respectively. As can be seen, there are three levels for each control factor, and there are only 2 levels for each noise factor. Based on these two tables, an OA $L_9(3^4)$ can be selected as the inner array, and an OA $L_8(2^7)$ can be selected as the outer array. The OAs can be found in a Statistical Software like SPSS.

Table VII lists the OA for this motor. The OA consists of an inner array with 9 combinations (as 9 rows) and an outer array with 8 combinations (as 8 columns on the right). The complete 8 combinations are 1111, 1112, 1221, 1222, 2121, 2122, 2211 and 2212, where 1 or 2 represents the level of the noise factor. Please note only the first and the last combinations are listed in the OA due to the limited space. Therefore, 72 (9×8) combinations will be required as the samples of this Taguchi design. They are located in the bottom right corner of the table with double solid lines.

Step 2: Calculate the response of all 72 (9×8) samples. By using 3-D FEM and thermal network model, all motor performance parameters listed in (6) can be computed. For example, the output powers of the first and last columns (18 values in total) are listed in Table VII. Then, the objective values can be obtained. Please note that constraints are normally not considered in the Taguchi design [19-24]. When the constraints are ignored and conventional Taguchi design is applied, the PoF of the optimal design is always big. To solve this problem, a penalty objective function is defined as follows.

$$y_{i,j} = f(x_{i,j}) + 1000 \sum_{k=1}^{5} u(g_{i,j}) \quad (7)$$

where i (1,2,…,9) and j (1,2,…,8) are the indices of the considered control and noise factor, respectively, as shown in Table VII. $u(g_{i,j}) = 1$ if $g_{i,j} > 0$, otherwise, it is 0.

Step 3: Calculate the SNR and average SNR for each level of every control factor. As the design target is the smaller the better, the SNR calculation equation of this motor is

$$\mathrm{SNR}(i) = -10 \log\left(\frac{1}{8}\sum_{j=1}^{8} y_{i,j}^2\right). \quad (8)$$

The average SNR of a level of a parameter can be calculated based on these SNRs and Table VII. For example, the average SNR for the first level of the second factor (H_{pm}) can be computed as

$$\overline{\mathrm{SNR}}(H_{pm}, 1) = \frac{\mathrm{SNR}(1)+\mathrm{SNR}(4)+\mathrm{SNR}(7)}{3} = -21.85\ dB\ , \quad (9)$$

where the numbers 1, 4, and 7 are the positions of level 1 for the second factor (H_{pm}) in Table VII. Average SNRs for other parameters and respective levels can be calculated in a similar way. Figure 8 shows the average SNRs for all control factors.

Step 4: Determine the best factor-level combination. As the design target is the smaller the better, the best level of each factor is the one that has the highest SNR. As shown in Fig. 8, levels 3, 1, 1, 2 are the best for the four control factors, respectively. The motor performance of this design is listed in Table VIII. As shown, the output power is 568.9 W, which is higher than the value (500 W) of the initial design, the material cost is AUD 13.04, which is smaller than that (AUD 16.46) of the initial design. Thus, the motor performance can be improved by using Taguchi design approach. Table IX lists the probability values for each constraint and the final motor PoF for this design. For the evaluation, MCA with 10,000 points was employed. As shown in the table, the probability of each constraint to be fulfilled is 1 or 100%. Thus, the PoF of this motor with the optimal Taguchi design listed in Table VIII is 0 (or the reliability is 100% in terms of the defined five constraints).

TABLE V
LEVELS OF CONTROL FACTORS

Control Factor	Unit	Level		
		1	2	3
W_{pm}	deg	11	11.5	12
H_{pm}	mm	11	11.5	12
N	turns	77	80	83
D	mm	1.0	1.1	1.2

TABLE VI
LEVELS OF NOISE FACTORS

Noise Factor	Unit	Level	
		1	2
W_{pm}	deg	-0.05	+0.05
H_{pm}	mm	-0.05	+0.05
N	turns	-0.5	+0.5
D	mm	-0.01	+0.01

TABLE VII
OA AND OUTPUT POWER RESPONSE

	Inner Array $L_9(3^4)$ (control factors)				**Outer Array $L_8(2^7)$** (noise factors)		
No	**1**	**2**	**3**	**4**	**1111**	**…**	**2212**
1	1	1	1	1	524.5	…	532.8
2	1	2	2	2	570.2	…	578.7
3	1	3	3	3	616.8	…	625.6
4	2	1	2	3	568.6	…	577.0
5	2	2	3	1	616.6	…	625.2
6	2	3	1	2	586.9	…	594.7
7	3	1	3	2	611.0	…	619.6
8	3	2	1	3	583.2	…	590.9
9	3	3	2	1	631.5	…	639.5

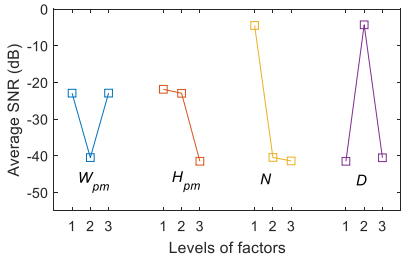

Fig. 8. Average SNRs for all factors

TABLE VIII
PERFORMANCE COMPARISON OF DIFFERENT OPTIMAL ROBUST DESIGNS

Par.	Unit	DA	Taguchi	WC	DFSS
W_{pm}	deg	10.15	12.00	10.15	10.60
H_{pm}	mm	11.00	11.00	11.00	11.45
N	turns	97	77	94	82
D	mm	1.08	1.10	1.08	1.09
Cost	AUD	11.96	13.04	11.89	12.36
P_{out}	W	645.5	568.9	623.2	575.5
η	%	84.96	83.74	84.64	83.84
sf	-	0.70	0.57	0.68	0.60
T_{coil}	℃	75.0	71.4	74.1	71.9
T_{pm}	℃	58.1	56.5	57.5	56.6
Obj.	-	1.50	1.67	1.52	1.62

TABLE IX
RELIABILITY OF CONSTRAINTS AND POF OF MOTOR FOR DIFFERENT DESIGNS

	DA	Taguchi	WC	DFSS
g_1	1	1	1	1
g_2	1	1	1	1
g_3	0.676	1	1	1
g_4	0.531	1	1	1
g_5	1	1	1	1
PoF	0.641	0	0	0

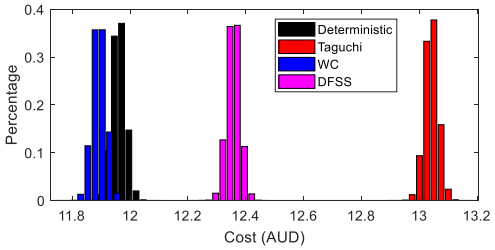

Fig. 9. Distributions of material cost after MCA for different designs.

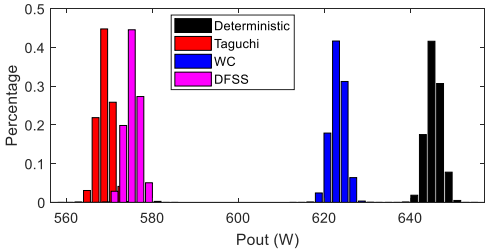

Fig. 10. Distributions of output power after MCA for different designs.

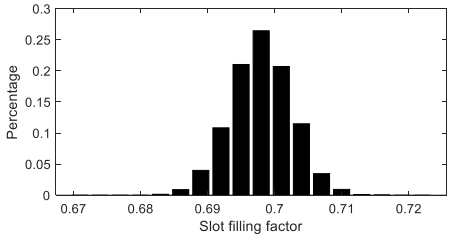

Fig. 11. Distribution of the slot filling factor for the design obtained by the deterministic approach.

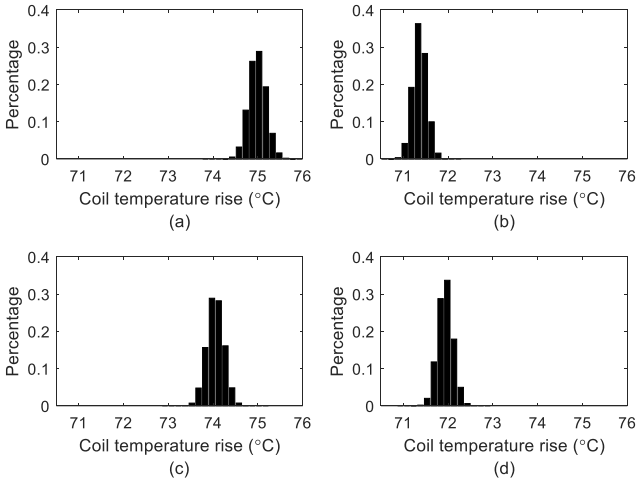

Fig. 12. Distributions of coil temperature rise for different designs, (a) deterministic, (b) Taguchi, (c) WC, and (d) DFSS in the presence of uncertainties.

C. Optimization Process and Results of WC Approach

The optimization process of WC approach includes the following three steps.

Step 1: Construct the WC optimization model. Based on (3) and (6), the WC optimization model can be expressed as

$$\begin{aligned} \min:\quad & f_w(\mathbf{x}) = \max_{\boldsymbol{\xi}\in U(\boldsymbol{\xi})} f(\mathbf{x},\boldsymbol{\xi}) \\ \text{s.t.}\quad & g_{w,j}(\mathbf{x}) = \max_{\boldsymbol{\xi}\in U(\boldsymbol{\xi})} g_j(\mathbf{x},\boldsymbol{\xi}) \le 0, j = 1,2,\dots,5 \\ & U(\boldsymbol{\xi}) = \{\boldsymbol{\xi}\in R^4 | \Delta\boldsymbol{\xi} = [0.05, 0.05, 0.5, 0.01]^T\} \end{aligned} \tag{10}$$

where design variables ($\mathbf{x}$) and noise factors ($\boldsymbol{\xi}$) are the same 4 parameters listed in Table III, $\Delta\boldsymbol{\xi}$ is defined in Table VI.

Step 2: Develop the Kriging model for the corresponding 3-D FEM. In the implementation, a five-level full-factor design is applied to parameters W_{pm} and H_{pm}. Thus, 25 samples will be simulated and the Kriging model will be developed based on these samples. As the performance of this motor is calculated based on 3-D FEM, it is very time-consuming if FEM is used in the optimization. Thus, Kriging model is used in this work to replace the FEM. Kriging model has been widely used as an approximation model in the design optimization of electromagnetic devices. The formulations and advantages of Kriging model can be found in [2,5,38,39].

Step 3: Optimize the model (10) based on Kriging models. Many optimization algorithms can be used, such as genetic algorithm or differential evolution algorithm (DEA). DEA is used in this work. Its details can be found in [2]. The optimization results are listed in Table VIII. The corresponding probability of each constraint and the motor PoF are listed in Table IX. As can be observed, PoF of 0 is obtained for this approach. A comparison of all approaches will be conducted in subsection E.

D. Optimization Process and Results of DFSS Approach

The optimization process of DFSS approach is similar to that of WC, except for two aspects. The first aspect is the construction of the robust optimization model. Based on (4) and (6), the DFSS optimization model can be expressed as

$$\begin{aligned} \text{min:} \quad & \mu[f(\mathbf{x})] \\ \text{s.t.} \quad & \mu[g_j(\mathbf{x})] + 6\sigma[g_j(\mathbf{x})] \le 0, j = 1,2,\dots,5 \end{aligned} \tag{11}$$

Please note that there are several forms for this objective function, like $\mu[f(\mathbf{x})] + \sigma[f(\mathbf{x})]$ and $\sigma[f(\mathbf{x})]/\mu[f(\mathbf{x})]$. As the average performance is used in the Taguchi method, $\mu[f(\mathbf{x})]$ is defined in (11) to make a fair comparison of the different methods. Nevertheless, comparisons for alternative formulations could be considered either.

The second aspect is the distributions of the noise factors. For WC approach, only the range of each noise factor is required. For the DFSS approach, a probability distribution function is required for each noise factor. The noise factors in electrical machines are mainly related to the manufacturing tolerances which are random in the manufacturing process, like the dimension of PM. Therefore, they are usually defined to follow normal distributions [28,29]. For a specific application, it is possible to have a noise factor following another distribution. This may affect the distributions of the objectives. Therefore, a distribution map with frequency is clearer to show the performance variations under uncertainties compared with single-valued distribution quantities like the mean.

For the investigated motor, it is reasonable to take normal distributions for those noise factors from previous studies [2,3,29]. The optimization results given by DEA and the corresponding probability and PoF are tabulated in Tables VIII and IX as well.

E. Comparison and Discussions

The optimization results of the deterministic approach (DA column) are listed in Tables VIII and IX as well for comparison. Figures 9 and 10 show the distributions of material cost and output power, respectively, for different robust designs after MCA. Form these figures and Tables VIII and IX, the following conclusions can be drawn:

First, the motor performance of all robust designs are better than that of the initial design, for example, the output powers are exceeding 500 W. However, they are slightly worse than for the design obtained by the deterministic approach. The objective value for that design is 1.50, which is the smallest one among them.

Second, the PoF values of all Taguchi design, WC and DFSS are zero, while the PoF of deterministic design is 64.1%. Thus, the smallest objective value of deterministic design is obtained at the cost of high PoF. The reason for this fact is that the reliabilities of the third and fourth constraints are less than 1. As shown, the nominal values for the slot filling factor and winding temperature rise of the optimal deterministic design are 0.70 and 75.0 ℃, respectively, which are equal to the permitted limits (0.7 and 75 ℃). This is the nature of deterministic design,. As they are obtained without the consideration of the uncertainties, the practical values obtained in the presence of inevitable uncertainties will have an increased risk of violating the limit. To have a clear understanding, Fig. 11 illustrates the distribution of the slot filling factor (third constraint) after MCA. As shown, many practical design points (considering uncertainties) are over the limit of 0.7. Figure 12 illustrates the distributions of the temperature rise in the winding (the fourth constraint) for all four optimal designs. Similarly, some points of the deterministic approach are over the limit of 75 ℃. For all three robust designs, the temperature is below the limit for any variation. Thus, deterministic design tends to have high PoF.

Third, it can be observed that the optimal Taguchi design highly depends on the selected levels of control factors listed in Table V. Table X lists another attempt where the second level of each factor is selected as the value for the initial design (this is quite reasonable). After a similar process, the best combination of control factor levels and the corresponding motor performance and PoF are listed in Table XI. Similarly, motor performance has been improved. However, please note that the temperature rise in the winding of this design is 84.2 ℃, which is much higher than the limit, 75 ℃. The corresponding PoF is 1 or 100%. Therefore, a good Taguchi design requires some useful prior information or experience for the determination of the levels of control factors.

TABLE X
CONTROL FACTORS OF TAGUCHI DESIGN – ANOTHER ATTEMPT

Control Factor	Unit	Level			Best level
		1	2	3	
W_{pm}	deg	11.5	12	12.5	11.50
H_{pm}	mm	14.5	15	15.5	14.50
N	turns	72	75	78	78
D	mm	1.0	1.1	1.2	1.00

TABLE XI
PERFORMANCE AND POF OF TAGUCHI DESIGN – ANOTHER ATTEMPT

Par.	Unit	Value	Reliability	Value
Cost	AUD	15.26	g_1	1
P_{out}	W	697.7	g_2	1
η	%	84.42	g_3	1
sf	-	0.49	g_4	0
T_{coil}	℃	84.2	g_5	1
T_{pm}	℃	66.6	PoF	1

IV. SPACE REDUCTION OPTIMIZATION STRATEGY FOR ROBUST DESIGN OPTIMIZATION

There are two main reasons for proposing a space reduction technique here. First, as discussed in the last section, Taguchi design approach is a very powerful robust design tool. However, it cannot handle design spaces with large number of dimensions efficiently and its effectiveness highly depends on the control factor levels (requiring experience about the optimization problem). Second, for the high-dimensional case, the WC and DFSS methods based on Kriging model are not efficient or applicable either. For example, if 7 parameters with 5 levels each are considered for evaluation by FEM, the number of required FEM samples is huge, i.e. 5^7 =78,125 samples, which is a huge computational burden as 3-D FEM is required and both alternating and rotational core losses are calculated (several minutes are required for one sample or design candidate when evaluating it by using *ANSYS*.

To attempt these two problems, a space reduction optimization (SRO) strategy is proposed in this section. Figure 13 shows the flowchart of the proposed strategy. The main idea is that the initial design space is normally quite large while the final optimal design is typically located in a small subspace of the initial design space. If an appropriate space reduction method can be developed to reduce the space first, the overall optimization efficiency is improved.

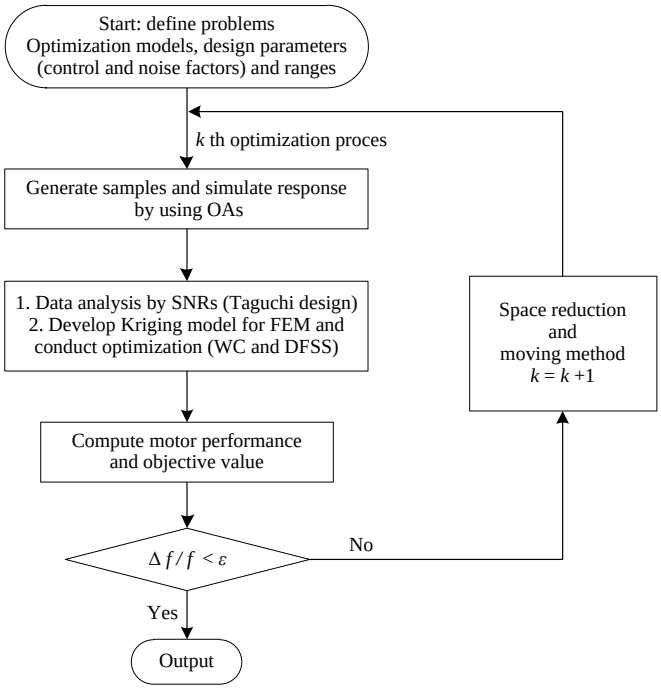

Fig. 13. A flowchart of the space reduction optimization strategy

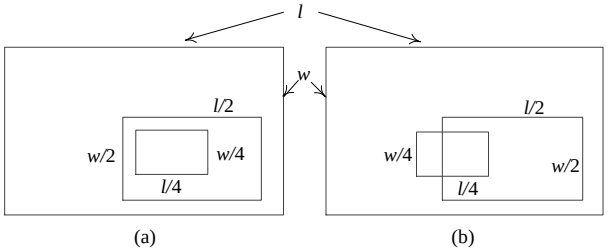

Fig. 14. Illustrations of space reduction method with three reduction steps, (a) reduction only, and (b) reduction with moving

Figure 14 illustrates the main idea of the space reduction method in the SRO strategy. In the implementation of SRO, there are five main steps.

Step 1: Define the robust optimization models, including objective functions, constraints, design parameters (control and noise factors) and their ranges (or the initial design space) for the investigated electrical machine.

Step 2: Generate samples and simulate their response. For Taguchi design approach, an OA is required in this step. For WC and DFSS, the following sampling strategy is used. First, divide all parameters into two groups by using sensitivity analysis results and assign them to two subspaces, significant parameter space and non-significant parameter space. For the sensitivity analysis, several methods can be employed, such as local sensitivity analysis method, global sensitivity analysis method, and analysis of variance. The implementation of them including the selection of factor levels can be found in reference [6]. Second, apply different levels to two groups. An OA with a higher level like 5 levels can be assigned to the first subspace, while a smaller level, like 3 levels, can be applied to the second group. Third, combine them to generate the samples for WC and DFSS approaches.

Step 3: Analyze the data by using SNRs or optimize the models by using Kriging model. For the Taguchi method, only SNR is required to obtain the best factor-level combination of control factors. For the WC and DFSS, develop a Kriging model based on the data first. Then, conduct the optimization by using DEA to gain optimization results. Last, calculate the motor performance, objective value and PoF for the optimal designs.

Step 4: Compute the motor performance with the obtained optimal design and compare it with the last objective. If the relative error between them is less than ε (a positive value like 1%), finish the optimization process and output the obtained optimal design. Otherwise, go to the next step and re-implement steps 2 and 3.

Step 5: Reduce the design space of the control factors by using the optimal design. The space reduction method is defined as follows. Assume the initial design space of a control factor is $[a, b]$, and there are three levels with a step size $2d$. If the optimal value of this factor is x_o, then the design space and new levels in the next iteration process are

$$\begin{cases} [a,\ a+d,\ a+2d] & x_o - d < a \\ [b-2d,\ b-d,\ b] & x_o + d > b \\ [x_o - d,\ x_o,\ x_o + d] & others \end{cases} \quad (12)$$

If there are four levels for each design parameter, the design space and new levels in the next iteration process are

$$\begin{cases} [a, a+d, a+2d, a+3d] & x_o - 3d/2 < a \\ [b-3d, b-2d, b-d, b] & x_o + 3d/2 > b \\ [x_o - \frac{3}{2}d, x_o - \frac{1}{2}d, x_o + \frac{1}{2}d, x_o + \frac{3}{2}d] & others \end{cases} \quad (13)$$

If there are five levels for each design parameter, the design space and new levels in the next iteration process are

$$\begin{cases} [a, a+d, a+2d, a+3d, a+4d,] & x_o - 2d < a \\ [b-4d, b-3d, b-2d, b-d, b] & x_o + 2d > b \\ [x_o - 2d, x_o - d,\ x_o,\ x_o + d, x_o + 2d] & others \end{cases} \quad (14)$$

As shown in (12)-(14), the design space can be halved by using this space reduction strategy. This will speed up the optimization process. Similar strategy has been proposed for Taguchi design method in the previous work and good robust designs have been obtained [40,41]. This work extends it to the WC and DFSS by using a new sampling strategy for the samples of Kriging model.

V. Comparison of Robust Design Optimization Methods with SRO Strategy

This section compares the performance of the three robust design approaches without and with SRO strategy. The first two subsections present low-dimensional and high-dimensional case studies, respectively. The last subsection presents a comparison for all robust design optimization methods.

A. Low-Dimensional Design Case

For the low-dimensional design example, as discussed in section III, WC and DFSS approaches can present good designs while Taguchi design has two problems (as mentioned in section III.E). To solve these problems, SRO strategy is applied

to the conventional Taguchi design with the initial design space. Thus, the same initial design space applies to all Taguchi, WC and DFSS method. Table XII lists the optimization results and motor performance. As can be seen, the motor performance has been improved and the PoF is 0. As a comparison, Fig. 15 shows the distribution of winding temperature rise after MCA. As shown, all points are below the limit. Figure 16 illustrates the iteration process of Taguchi design with SRO. As shown, six iterations are required for the convergence of the proposed SRO. Each iteration requires 72 points, so 422 FEM simulations in total. In this case, WC and DFSS are more efficient. In the iteration process, though two designs (k=1,3 as shown in Fig. 16) do not satisfy the constraints, the others are good. Thus, the proposed method is efficient and robust.

TABLE XII
TAGUCHI DESIGN WITH SRO FOR LOW-DIMENSIONAL CASE

Par.	Vlaue	Par.	Value	Prob.	Value
W_{pm}	10.57	η	83.09	g_1	1
H_{pm}	12.98	sf	0.53	g_2	1
N	73	T_{coil}	73.4	g_3	1
D	1.08	T_{pm}	58.4	g_4	1
$Cost$	13.26	Obj	1.70	g_5	1
P_{out}	559.7			PoF	0

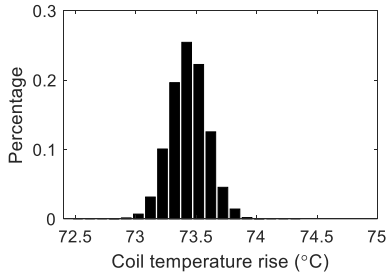

Fig. 15. Distribution of coil temperature rise for Taguchi design with SRO for low dimensional case

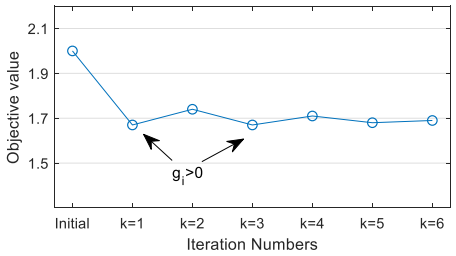

Fig. 16. Iteration process of Taguchi method with SRO for low dimensional case

B. *High-Dimensional Design Case*

Table XIII lists the nine parameters to be considered in this case. For the optimization, six parameters will be considered as control factors, and they are W_{pm}, H_{pm}, N, D, W_{st}, H_{st}. Among them, W_{pm} and H_{pm} are related to the rotor, W_{st} and H_{st} are related to the SMC stator, and N and D are winding parameters, as defined in Table II. The other three parameters, L_{gap}, B_r, ρ, are considered as noise factors only. From previous research, it is found that L_{gap}, B_r, ρ, are very important to motor performance. The ranges of these three parameters are determined by previous experimental results [30]. Due to the small ranges of them, they are assigned to the non-significant subspace as only 3 levels are required. Please note that W_{pm}, H_{pm}, N, D, are considered as noise factors as well. Thus, there are 6 control factors and 7 noise factors for this example.

Seven approaches are discussed and compared in this case, as they are the deterministic, conventional Taguchi, Taguchi with SRO strategy, WC, WC with SRO strategy, DFSS, and DFSS with SRO strategy approach.

For the conventional Taguchi approach, Tables XIV and XV list the control factors and noise factors, respectively, and their levels. As shown, 5 levels are defined for each control factor, and 2 levels are defined to each noise factor. The levels of noise factors are mainly defined based on our previous work on SMC motors. For example, the levels of the remanence of PM and the core density are chosen based on previous experimental results [30].To implement the Taguchi design, an OA $L_{25}(5^6)$ is defined as the inner array, and $L_8(2^7)$ is selected as the outer array, so 200 FEM simulations (25×8) are required (this process is similar to the analysis steps 1 and 2 in section III.B). For the Taguchi design with SRO strategy, Table XVI lists the control factors and their levels for the first iteration of the SRO. As shown, the levels completely cover the big initial design space defined in Table XIII. This is the difference between Tables XIV and XVI. Table XVII tabulates the optimization results for these seven approaches. Table XVIII lists the probability values for all constraints and the PoF values for the motor.

TABLE XIII
DESIGN PARAMETERS AND RANGES FOR HIGH-DIMENSIONAL CASE

Par.	Unit	Initial	Min	Max	Step Size
W_{pm}	deg	12	10	14	0.05
H_{pm}	mm	15	11	17	0.05
N	turns	75	60	100	1
D	mm	1.1	0.9	1.5	0.01
W_{st}	mm	8	7	10	0.05
H_{st}	mm	14.35	10	16	0.05
L_{gap}	mm	1	0.95	1.05	-
B_r	T	1.15	1.10	1.20	-
ρ	g/mm^3	7.32	7.17	7.47	-

TABLE XIV
LEVELS OF CONTROL FACTORS FOR HIGH-DIMENSIONAL CASE

Control Factor	Unit	Level				
		1	2	3	4	5
W_{pm}	deg	7.60	7.80	8.00	8.20	8.40
H_{pm}	mm	11.00	11.50	12.00	12.50	13.00
N	turns	69	72	75	78	81
D	mm	0.90	1.00	1.10	1.20	1.30
W_{st}	mm	13.85	14.10	14.35	14.60	14.85
H_{st}	mm	14.00	14.50	15.00	15.50	16.00

TABLE XV
LEVELS OF NOISE FACTORS FOR HIGH-DIMENSIONAL CASE

Noise Factor	Unit	Level	
		1	2
W_{pm}	deg	-0.05	+0.05
H_{pm}	mm	-0.05	+0.05
N	turns	-0.5	+0.5
D	mm	-0.01	+0.01
L_{gap}	mm	-0.05	+0.05
B_r	T	-0.05	+0.05
ρ	g/mm^3	-0.15	+0.15

TABLE XVI
LEVELS OF CONTROL FACTORS FOR TAGUCHI DESIGN WITH SRO STRATEGY

Control Factor	Unit	Level				
		1	2	3	4	5
W_{pm}	deg	10	11	12	13	14
H_{pm}	mm	11	12.5	14	15.5	17
N	turns	60	70	80	90	100
D	mm	0.9	1.05	1.2	1.35	1.5
W_{st}	mm	7	7.8	8.6	9.2	10
H_{st}	mm	10	11.5	13	14.5	16

TABLE XVII
PERFORMANCE COMPARISON OF DIFFERENT ROBUST METHODS FOR HIGH-DIMENSIONAL CASE

Par.	Unit	DA	Tag.	Tag. SRO	WC	WC SRO	DFSS	DFSS SRO
W_{st}	mm	7.35	8.20	7.95	7.10	7.00	7.00	7.30
W_{pm}	deg	10.15	11.00	11.75	10.10	10.00	10.00	10.00
H_{st}	mm	12.40	14.35	10.00	11.25	11.45	11.10	10.95
H_{pm}	mm	11.05	14.50	13.25	11.05	11.45	11.05	11.05
N	turns	100	69	73	96	94	95	96
D	mm	1.06	1.20	1.13	1.07	1.08	1.07	1.07
$Cost$	AUD	11.88	15.16	14.63	11.75	11.99	11.64	11.68
P_{out}	W	675.5	589.8	540.7	618.2	617.2	600.6	606.8
η	%	85.79	83.64	84.37	85.49	85.54	85.32	85.36
sf	-	0.70	0.61	0.57	0.68	0.68	0.67	0.68
T_{coil}	℃	74.9	73.2	65.8	70.7	70.0	69.8	70.1
T_{pm}	℃	68.5	70.6	62.2	64.8	64.5	63.9	64.1
F	-	1.46	1.77	1.81	1.52	1.54	1.54	1.53
FEM	-	~9k	200	600	>10k	675	>10k	450

TABLE XVIII
PROBABILITY AND POF VALUES FOR HIGH-DIMENSIOANL CASE

	DA	Tag.	Tag. SRO	WC	WC SRO	DFSS	DFSS SRO
g_1	1	1	1	1	1	1	1
g_2	1	1	1	1	1	1	1
g_3	0.866	1	1	1	1	1	1
g_4	0.541	0.963	1	1	1	1	1
g_5	1	1	1	1	1	1	1
PoF	0.532	0.037	0	0	0	0	0

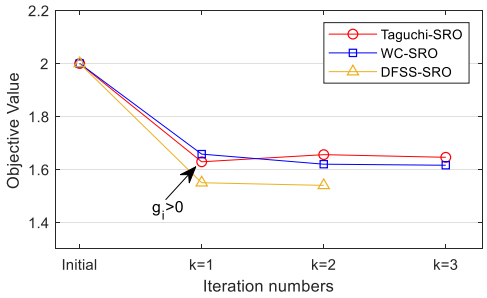

Fig. 17. Iteration process of the proposed SRO strategy for robust methods

Figure 17 shows the iteration process for the three robust design optimization methods with SRO. As shown, only 2 or 3 iterations are required for them. Thus, the proposed method is efficient. Figures 18 and 19 illustrate the distributions of the material cost and output power of all seven optimal designs after MCA. The following conclusions can be drawn:

Firstly, regarding the motor performance and objective value, all robust designs are better than those of the initial design. The deterministic design is the best among them, and it has the smallest objective value, 1.46. The WC and DFSS (with and without SRO) have similar objective values (in the range of 1.52 to 1.54) and motor performance. The objective values of two Taguchi designs are larger, around 1.80.

Secondly, regarding the PoF of the motor in production with these designs, the PoF of deterministic design is 53.2%, the PoF of conventional Taguchi design 3.7%, while the others are zero. Thus, the cost of the minimal objective of deterministic design is the highest PoF, which is unacceptable from the perspective of industrial design and production. As an illustration of the PoF, the distributions of the temperature rise in the winding (the fourth constraint) of seven designs are illustrated in Fig. 20. As shown, some points in the deterministic and Taguchi approaches are violating the limit. Thus, its PoF is higher than zero.

Thirdly, regarding the computation cost, deterministic approach requires around 9,000 FEMs (45×200, where 45 is the population size for each generation and 200 is the average number of generations for DEA), the FEM samples required by WC and DFSS are more than 10,000 (for the development of a sufficiently accurate Kriging model), which represent huge computational cost. For the conventional Taguchi design, only 200 FEMs are required, which is the smallest one among all seven different approaches. The required FEM samples for Taguchi with SRO strategy are 600, which is higher than the ones required by the conventional Taguchi design. However, the PoF of the optimal design is 0, which is much more reasonable. Also, this method does not require any prior information for the levels of the control factors. The FEM samples required by WC and DFSS with SRO strategy are 675 and 450, respectively, which are less than 10% of those required by the conventional WC and DFSS. Furthermore, both WC and DFSS combined with SRO can provide optimal designs of similar performance when compared with the classical computationally costly approaches without SRO. Therefore, the proposed SRO is very efficient for all three robust design optimization methods.

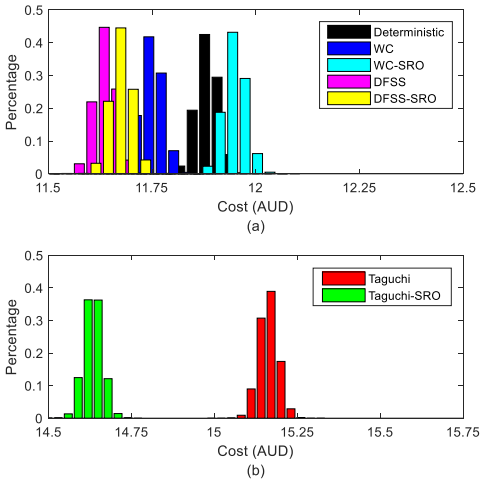

Fig. 18. Distributions of material cost for different methods

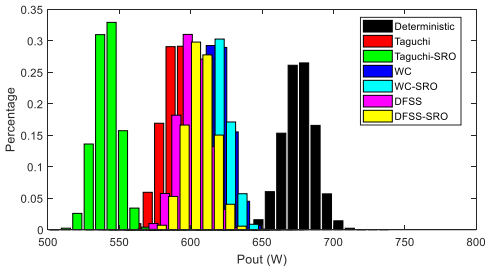

Fig. 19. Distributions of output power for different methods

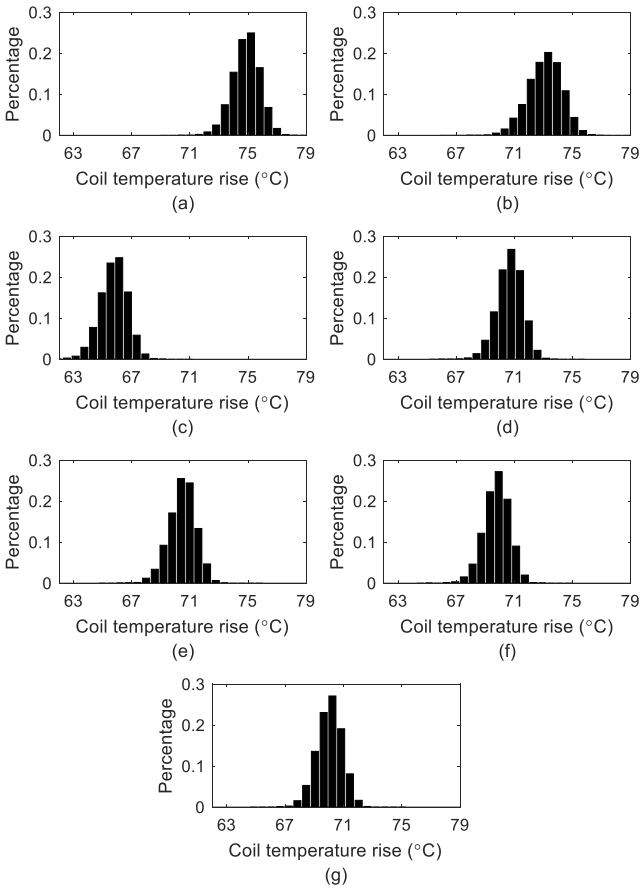

Fig. 20. Distributions of coil temperature rise for seven designs, (a) deterministic, (b) Taguchi, (c) Taguchi with SRO, (d) WC, (e) WC with SRO, (f) DFSS, and (g) DFSS with SRO

C. Comparison of Robust Design Optimization Methods

Table XIX summaries the comparison of six types of robust design optimization methods, the conventional Taguchi design, WC design and DFSS, Taguchi design with SRO strategy, WC with SRO and DFSS with SRO methods. The three SRO robust approaches are combined in one column in the table. These methods are compared in terms of ten aspects, such as the applicable dimensionality (low or high) and the overall design space size (small or big).

Regarding the conventional Taguchi design method, it can be easily applied to high-dimensional problems and requires small FEM samples. However, it is hard to handle the constraints and wide design spaces, and the optimal design's PoF highly depends on the initially selected levels of control factors.

Regarding the conventional WC and DFSS methods, they have similar advantages, like easy to handle constraints and smaller PoF. However, they are more efficient for the low-dimensional case and require huge computation cost for the high-dimensional case. The main difference between them is that for DFSS the distribution type of the noise factors is required, while for WC it is not. Also, as WC is a minimax problem, the optimization process usually takes more time than DFSS.

Regarding the three robust design optimization methods with SRO strategy, they have the advantages of all the conventional methods and their disadvantages are significantly reduced. They can be applied to high-dimensional optimization scenarios with comparably low computation cost.

Regarding the last aspect, multi-objective robust optimization, Taguchi design approach can hardly handle multi-objective optimization problems due to its limited number of levels. The WC and DFSS approaches do not feature this limitation. This aspect will be considered in another paper with a new optimization strategy.

TABLE XIX
COMPARSION OF DIFFERENT ROBUST DESIGN OPTIMIZATION METHODS

Aspect	Taguchi	WC	DFSS	SRO (Taguchi, WC, DFSS)
Dimension	low/high	low	low	high
Design space	small	big	big	big
Ability to handle constrains	not good	good	good	good
Experience for DoE samples	required	not required	not required	not required
Approximate model	no	yes	yes	yes
Optimal objective value	depends	smaller	smaller	smaller
PoF	depends	zero	zero	zero
Computation cost	low	high	high	low
distribution of uncertainty	no	no	yes	yes to DFSS only
Multiobjective application	hard	easy	easy	easy to WC & DFSS

VI. Conclusion

This paper presented an overview and comparative study for three popular robust design optimization methods, Taguchi parameter design, worst-case design and design for six-sigma. To efficiently attempt high-dimensional robust design optimization problems, SRO strategy was presented for all three robust design optimization methods. A design example was investigated for two different scenarios (low-dimensional and high-dimensional case) to compare the performance of different robust optimization methods in terms of the number of required design evaluations and achieved performance of the optimal design. From the comparison, it is found that applying the proposed SRO strategy allows for significantly minimizing the computational effort while achieving comparable results as obtained for the conventional robust design optimization methods. The proposed new methods are in particular very efficient for the high-dimensional robust optimization of electrical machines. In that case, they can provide similar optimal designs than the conventional worst-case and design for six-sigma approaches, but the required computational cost is less than 10 percent of the conventional approaches. Future work will be about more detailed studies of the proposed approaches featuring SRO and potential further improvements.

References

[1] G. Bramerdorfer, J. A. Tapia, J. J. Pyrhönen and A. Cavagnino, "Modern electrical machine design optimization: techniques, trends, and best practices," *IEEE Trans. Ind. Electron*., vol. 65, no. 10, pp. 7672-7684, Oct. 2018.

[2] G. Lei, J. G. Zhu, and Y. G. Guo, *Multidisciplinary Design Optimization Methods for Electrical Machines and Drive Systems*, Springer, ISBN: 978-3-662-49269-7, 2016.

[3] G. Lei, J. Zhu, Y. Guo, C. Liu and B. Ma, "A review of design optimization methods for electrical machines", *Energies*, vol. 10, no. 12, Art. no. 1962, pp. 1-31, Dec. 2017.

[4] D. Yao and D. M. Ionel, "A review of recent developments in electrical machine design optimization methods with a permanent magnet synchronous motor benchmark study", IEEE Trans. Industry Appl., vol. 49, no. 3, pp. 1268-1275, Sep. 2013.

[5] G. Lei, T. Wang, J. Zhu, et al., "System level design optimization method for electrical drive systems: deterministic approach," *IEEE Trans. Ind. Electron*., vol. 61, no. 12, pp. 6591-6602, 2014.

[6] G. Lei, C. Liu, J. Zhu, and Y. Guo, "Techniques for multilevel design optimization of permanent magnet motors," *IEEE Trans. Energy Convers*., vol. 30, no. 4, pp. 1574-1584, 2015.

[7] H. M. Hasanien, A. S. Abd-Rabou, and S. M. Sakr, "Design optimization of transverse flux linear motor for weight reduction and performance improvement using response surface model and genetic algorithm," *IEEE Trans. Energy Convers.*, vol. 25, no. 3, pp. 598-605, Sep. 2010.

[8] R. Nasiri-Zarandi, M. Mirsalim, and A. Cavagnino, "Analysis optimization and prototyping of a brushless DC limited-angle torque-motor with segmented rotor pole tip structure," *IEEE Trans. Ind. Electron.*, vol. 62, no. 8, pp. 4985-4993, Aug. 2015.

[9] X. Zhu, W. Wu, L. Quan, Z. Xiang and W. Gu, "Design and multi-objective stratified optimization of a less-rare-earth hybrid permanent magnets motor with high torque density and low cost," *IEEE Trans. Energy Convers*., vol. 34, no. 3, pp. 1178-1189, Sept. 2019.

[10] X. Zhao and S. Niu, "Design and Optimization of a novel slot-PM-assisted variable flux reluctance generator for hybrid electric vehicles," *IEEE Trans. Energy Convers*., vol. 33, no. 4, pp. 2102-2111, Dec. 2018.

[11] M. A. Khan, I. Husain, M. R. Islam, and J. T. Klass, "Design of experiments to address manufacturing tolerances and process variations influencing cogging torque and back EMF in the mass production of the PMSMs," *IEEE Trans. Ind. Appl.*, vol. 50, no. 1, pp. 346-355, 2014.

[12] A. J. Pina and L. Xu, "Analytical prediction of torque ripple in surface-mounted permanent magnet motors due to manufacturing variations," *IEEE Trans. Energy Convers.*, vol. 31, pp. 1634-1644, 2016.

[13] G. Bramerdorfer, "Tolerance Analysis for Electric Machine Design Optimization: Classification, Modeling and Evaluation, and Example," *IEEE Trans. Magn.*, vol. 55, no. 8, pp. 1-9, Aug. 2019, Art no. 8106809.

[14] G. Bramerdorfer, "Computationally Efficient Tolerance Analysis of the Cogging Torque of Brushless PMSMs," *IEEE Trans Ind. Appl*., vol. 53, no. 4, pp. 3387-3393, July-Aug. 2017.

[15] G. Bramerdorfer and A. Zăvoianu, "Surrogate-Based Multi-Objective Optimization of Electrical Machine Designs Facilitating Tolerance Analysis," *IEEE Trans. Magn.*, vol. 53, no. 8, pp. 1-11, Aug. 2017, Art no. 8107611.

[16] Y. Wang, S. Niu and W. Fu, "Sensitivity analysis and optimal design of a dual mechanical port bidirectional flux-modulated machine," *IEEE Trans. Ind. Electron*., vol. 65, no. 1, pp. 211-220, Jan. 2018.

[17] X. Ge and Z. Q. Zhu, "Influence of manufacturing tolerances on cogging torque in interior permanent magnet machines with eccentric and sinusoidal rotor contours," *IEEE Trans Ind. Appl*., vol. 53, no. 4, pp. 3568-3578, July-Aug. 2017.

[18] I. Coenen, M. Giet, and K. Hameyer, "Manufacturing tolerances: Estimation and prediction of cogging torque influenced by magnetization faults," *IEEE Trans. Magn.*, vol. 48, no. 5, pp. 1932-36, May 2012.

[19] J. Song, F. Dong, J. Zhao, S. Lu, S. Dou and H. Wang, "Optimal design of permanent magnet linear synchronous motors based on Taguchi method," *IET Electr. Power Appl.*, vol. 11, no. 1, pp. 41-48, 1 2017.

[20] F. Dong, J. Song, J. Zhao and J. Zhao, "Multi-objective design optimisation for PMSLM by FITM," *IET Electr. Power Appl.*, vol. 12, no. 2, pp. 188-194, 2 2018.

[21] S. Lee, K. Kim, S. Cho, J. Jang, T. Lee and J. Hong, "Optimal design of interior permanent magnet synchronous motor considering the manufacturing tolerances using Taguchi robust design," *IET Electr. Power Appl.*, vol. 8, no. 1, pp. 23-28, January 2014.

[22] K. S. Kim, K. T. Jung, J. M. Kim, J. P. Hong and S. I. Kim, "Taguchi robust optimum design for reducing the cogging torque of EPS motors considering magnetic unbalance caused by manufacturing tolerances of PM," *IET Electr. Power Appl*., vol. 10, no. 9, pp. 909-915, 11 2016.

[23] J. Tsai, C. Chang, W. Chen and J. Chou, "Optimal parameter design for IC wire bonding process by using fuzzy logic and Taguchi method," in IEEE Access, vol. 4, pp. 3034-3045, 2016.

[24] G. J. Park, T. H. Lee, K. Lee, K. H. Hwang, "Robust design: an overview," *AIAA Journal*, vol. 44, no. 1, pp. 181-191, 2016.

[25] Z. Ren, M. Pham and C. S. Koh, "Robust global optimization of electromagnetic devices with uncertain design parameters: comparison of the worst case optimization methods and multiobjective optimization approach using gradient index," *IEEE Trans. Magn.*, vol. 49, no. 2, pp. 851-859, Feb. 2013.

[26] Z. Ren, D. Zhang and C. Koh, "New reliability-based robust design optimization algorithms for electromagnetic devices utilizing worst case scenario approximation," *IEEE Trans. Magn.*, vol. 49, no. 5, pp. 2137-2140, May 2013.

[27] S. Xiao, Y. Li, M. Rotaru and J. K. Sykulski, "Six Sigma Quality Approach to Robust Optimization," *IEEE Trans. Magn.*, vol. 51, no. 3, pp. 1-4, March 2015, Art no. 7201304.

[28] P. N. Koch, R. J. Yang, and L. Gu. "Design for six sigma through robust optimization," *Struct. Multidiscip. Optim.*, vol. 26, no. 3-4, pp. 235-248, 2004.

[29] G. Lei, T. Wang, J. Zhu, Y. Guo, and S. Wang, "System-level design optimization method for electrical drive systems-robust approach," *IEEE Trans. Ind. Electron.*, vol. 62, no. 8, pp. 4702-4713, 2015.

[30] B. Ma, G. Lei, J. G. Zhu, Y. G. Guo and C. C. Liu, "Application-oriented robust design optimization method for batch production of permanent-magnet motors," *IEEE Trans. Ind. Electron*., vol. 65, no. 2, pp. 1728-1739, 2018.

[31] G. Lei, J. G. Zhu, Y. G. Guo, *et al.*, "Robust design optimization of PM-SMC motors for Six Sigma quality manufacturing," *IEEE Trans. Magn.*, vol. 49, no. 7, pp. 3953-3956, Jul. 2013.

[32] C. Liu, G. Lei, T. Wang, Y. Guo, Y. Wang, and J. Zhu, "Comparative study of small electrical machines with soft magnetic composite cores," *IEEE Trans. Ind. Electron.*, vol. 64, no. 2, pp. 1049-1060, 2017.

[33] A. Krings, A. Boglietti, A. Cavagnino and S. Sprague, "Soft magnetic material status and trends in electric machines," *IEEE Trans. Ind. Electron*., vol. 64, no. 3, pp. 2405-2414, March 2017.

[34] J. G. Zhu, Y. G. Guo, Z. W. Lin, Y. J. Li, and Y. K. Huang, "Development of PM transverse flux motors with soft magnetic composite cores," *IEEE Trans. Magn.*, vol. 47, no. 10, pp. 4376-4383, Oct. 2011.
[35] B. Ma, G. Lei, C. Liu, J. Zhu and Y. Guo, "Robust tolerance design optimization of a PM claw pole motor with soft magnetic composite cores," *IEEE Trans. Magn.*, vol. 54, no. 3, pp. 1-4, March 2018, Art no. 8102404.
[36] B. Ma, G. Lei, J. Zhu and Y. Guo, "Design optimization of a permanent magnet claw Pole motor with soft magnetic composite cores," *IEEE Trans. Magn.*, vol. 54, no. 3, pp. 1-4, March 2018, Art no. 8102204.
[37] Y. Huang, J. Zhu and Y. Guo, "Thermal analysis of high-speed SMC motor based on thermal network and 3-D FEA with rotational core loss included," *IEEE Trans. Magn.*, vol. 45, no. 10, pp. 4680-4683, Oct. 2009.
[38] S. N. Lophaven, H. B. Nielsen, and J. Sondergaard, "DACE: A MATLAB Kriging toolbox version 2.0," Technical Report IMM-TR-2002-12, Technical University of Denmark, Copenhagen, 2002.
[39] L. D. Wang and D. A Lowther, "Selection of approximation models for electromagnetic device optimization," *IEEE Trans. Magn.*, vol. 42, no. 2, pp. 1227-1230, Feb. 2006.
[40] C. Liu, G. Lei, B. Ma, Y. Guo, and J. Zhu, "Robust design of a low-cost permanent magnet motor with soft magnetic composite cores considering the manufacturing process and tolerances," *Energies*, vol. 11, no. 8, Art. no. 2025, 2018.
[41] G. Lei, C. Liu, Y. Li, D. Chen, Y. Guo and J. Zhu, "Robust design optimization of a high-Temperature superconducting linear synchronous motor based on Taguchi method," *IEEE Trans. Appl. Supercond.*, vol. 29, no. 2, pp. 1-6, March 2019, Art no. 3600206.

Gang Lei (M'14) received the B.S. degree in Mathematics from Huanggang Normal University, China, in 2003, the M.S. degree in Mathematics and Ph.D. degree in Electrical Engineering from Huazhong University of Science and Technology, China, in 2006 and 2009, respectively.

He is currently a Senior Lecturer at the School of Electrical and Data Engineering, University of Technology Sydney (UTS), Australia. His research interests include computational electromagnetics, design optimization and control of electrical drive systems and renewable energy systems. He is an Associate Editor of the IEEE TRANSACTIONS ON INDUSTRIAL ELECTRONICS.

Gerd Bramerdorfer (S'10-M'14-SM'18) received the Ph.D. degree in electrical engineering from Johannes Kepler University Linz, Linz, Austria, in 2014. He is currently an Assistant Professor with the Department of Electrical Drives and Power Electronics, Johannes Kepler University Linz. His research interests include the design, modeling, and optimization of electric machines as well as magnetic bearings and bearingless machines.

Dr. Bramerdorfer is a Senior Member of IEEE, an Editor of the IEEE TRANSACTIONS ON ENERGY CONVERSION and a past Associate Editor of the IEEE TRANSACTIONS ON INDUSTRIAL ELECTRONICS.

Chengcheng Liu (M'15) received the B.E. degree from the Yangzhou University, Yangzhou, China, in 2010, the Ph.D. degree from Hebei University of Technology, China, in 2015, all in electrical engineering.

He is currently a lecturer at the Hebei University of Technology, China. His research fields include the design, analysis and control of permanent magnet machines.

Youguang Guo (S'02-M'05-SM'06) received the B.E. degree from Huazhong University of Science and Technology, China in 1985, the M.E. degree from Zhejiang University, China in 1988, and the Ph.D. degree from University of Technology, Sydney (UTS), Australia in 2004, all in electrical engineering.

He is currently a Professor at the School of Electrical and Data Engineering, University of Technology Sydney (UTS). His research fields include measurement and modeling of properties of magnetic materials, numerical analysis of electromagnetic field, electrical machine design optimization, power electronic drives and control.

Jianguo Zhu (S'93–M'96–SM'03) received the B.E. degree in 1982 from Jiangsu Institute of Technology, Jiangsu, China, the M.E. degree in 1987 from Shanghai University of Technology, Shanghai, China, and the Ph.D. degree in 1995 from the University of Technology Sydney (UTS), Sydney, Australia, all in electrical engineering.

He was appointed a lecturer at UTS in 1994 and promoted to full professor in 2004 and Distinguished Professor of Electrical Engineering in 2017. At UTS, he has held various leadership positions, including the Head of School for School of Electrical, Mechanical and Mechatronic Systems and Director for Centre of Electrical Machines and Power Electronics. In 2018, he joined the University of Sydney, Australia, as a full professor and Head of School for School of Electrical and Information Engineering. His research interests include computational electromagnetics, measurement and modelling of magnetic properties of materials, electrical machines and drives, power electronics, renewable energy systems and smart micro grids.